AIAA 81-1945R

Stress Measurements in Bias-Constructed Parachute Canopies During Inflation and at Steady State

William L. Garrard* and Thomas A. Konicke†
University of Minnesota, Minneapolis, Minn.

This paper describes the results of an experimental study of canopy stresses in bias-constructed, solid-flat parachutes. Stresses were measured in the warp and fill directions during inflation and at steady state for different values of dynamic pressure. Omega sensors were used to measure stress. These sensors were mounted along the gore centerlines so that the warp and fill stress distributions could be determined as a function of distance from the vent. It was found that stresses in the fill direction were substantially larger than stresses in the warp direction.

Nomenclature

F_m = maximum force (drag) during inflation
F_{ss} = steady-state force (drag)
n = $\sigma_m/\sigma_{ss} \cdot F_{ss}/F_m$
q = dynamic pressure at inflated canopy
q^* = nominal dynamic pressure
R_0 = nominal radius of parachute
S = distance from apex measured along gore centerline
S^* = nondimensional distance, S/R_0
t = time of maximum stress
t_{f_m} = time of maximum drag
t^*_m = t/t_{f_m}
σ_m = maximum stress during inflation
σ_{ss} = steady-state stress

Introduction

THE objective of this study was to experimentally determine the canopy stress distribution in bias-constructed, solid-flat parachute models during inflation and at steady state. Stress measurements in block-constructed, solid-flat parachutes and in ringslot parachutes have been reported,[1,2] but only preliminary results on bias-constructed parachutes have appeared.[3] Since a large fraction of solid parachutes are bias constructed, it was felt that a more detailed study of the stress distribution in bias-constructed parachutes was required as an aid to the development of analytic design procedures for such parachutes.

Stress measurements were accomplished by use of Omega sensors. The Omega sensor, described in detail in the literature was developed at the University of Minnesota by the late Dr. H. G. Heinrich and has since been evaluated and used by several investigators.[1-6] If proper experimental techniques are followed, Omega sensors have been shown to be capable of providing accurate stress measurements in parachute canopies.[5]

Stress measurements were made on two circular solid-flat, bias-constructed model parachutes. On each parachute, Omega sensors were mounted along the gore centerlines and stresses in both warp and fill directions were measured as the parachutes were inflated in the wind tunnel. Warp refers to the threads that run parallel to the edge of the cloth. Fill refers to the threads that run perpendicular to the warp threads. In bias-constructed parachutes these threads intersect the gore centerline at an angle of 45 deg. It was found that the stresses in the fill direction were significantly larger than the stresses in the warp direction. To the authors' knowledge, this is a new result. It is hypothesized that the difference in stress in the warp and fill directions is due to the anisotropic stress/strain characteristics of the parachute cloth.

Received Sept. 22, 1980; revision received March 6, 1981; presented as Paper 81-1945 at the AIAA 7th Aerodynamic Decelerator and Balloon Technology Conference, San Diego, Calif., Oct. 21-23, 1981.
Copyright © American Institute of Aeronautics and Astronautics, Inc., 1981. All rights reserved.

*Associate Professor, Department of Aerospace Engineering and Mechanics. Associate Fellow AIAA.
†Research Assistant, Department of Aerospace Engineering and Mechanics. Student Member AIAA.

Experimental Design and Test Procedure

The two parachute models used had a diameter of 4 ft (1.22 m) and were made up of 24 gores. The canopies were constructed of 1.1 oz/yd^2 (37.375 gm/m^2) rip stop nylon cloth, type MIL-C7020-1, with an effective porosity of 4%. The number of yarns per inch and the nominal ultimate breaking strength in the warp and fill directions are the same for this cloth. One hundred pound (446 N) test nylon cord was used for suspension lines. Construction followed the specifications in Ref. 7. One parachute was constructed of orange cloth, the other of white cloth; hence the parachutes are called the orange parachute and the white parachute. Except for color, the two parachutes were of identical design.

Tests were conducted in the open section of the University of Minnesota low-speed wind tunnel. A maximum dynamic pressure of approximately 10 psf (478.8 Pa) was obtainable in this portion of the wind tunnel. The nominal dynamic pressure (q^*) was measured approximately 3 ft (1 m) upstream from the canopy. The dynamic pressure at the canopy location (q) was approximately 15% lower than the nominal. The dynamic pressure dropped an additional 8% upon inflation of the parachute. All reported dynamic pressures are nominal pressures read before inflation.

The Omega sensors used for stress measurement have been extensively discussed in the literature.[1-3,5] A total of 33 sensors were mounted on the outside of the two parachutes. Twelve sensors were placed along the gore centerlines of the orange parachute at S^* values of 0.2, 0.4, 0.6, 0.8, 0.9, and 0.96. Six of these sensors measured stress in the warp direction and six measured stress in the fill direction. Five additional sensors were mounted in the fill direction in different gores at an S^* of 0.6 in order to determine the stress variation from gore to gore. The value of 0.6 was selected since the stress level was reasonably large and the date scatter was small at this point. All the Omega sensors on the white parachute were placed in the fill direction. It was originally planned to make warp and fill measurements on both parachutes, but, as discussed below, the variations in fill stress from gore to gore were so large for the white parachute that no warp stresses were measured on this parachute. Sensors were located at S^* values of 0.2, 0.3, 0.6, 0.8, 0.9, and 0.96. As in the case of the orange parachute, five additional sensors were mounted in different gores at an S^* of 0.6.

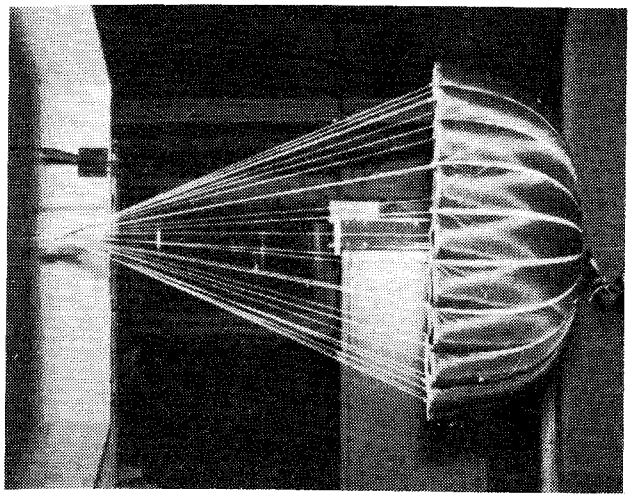

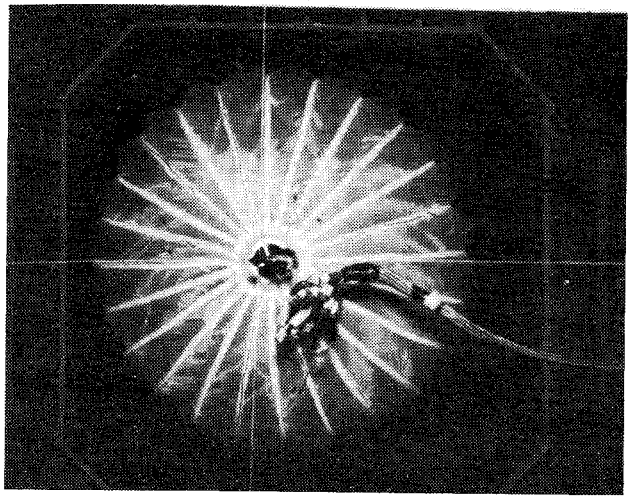

Fig. 1 Side and upstream view of the orange parachute in a wind tunnel at 5.3 psf (q^*).

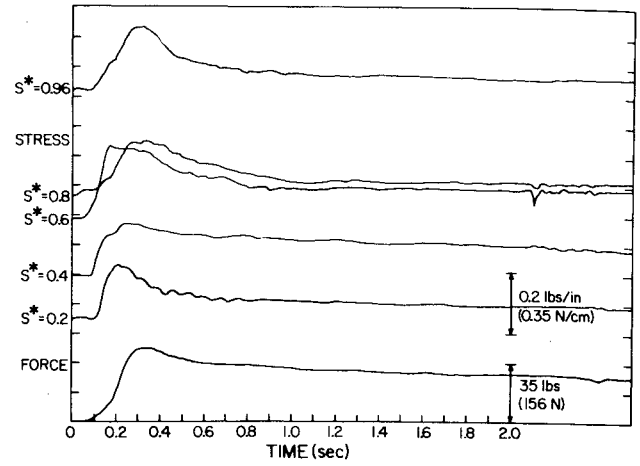

Fig. 2 Typical time history of stress and drag force at 5.3 psf (q^*).

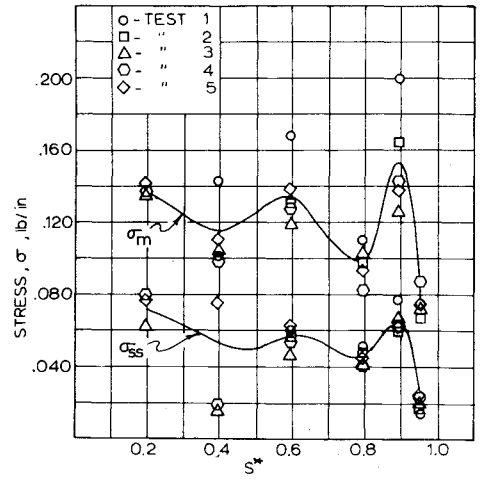

Fig. 3 Maximum and steady-state stress distributions measured on the orange parachute at 5.3 psf (q^*) in the warp direction.

A sting held the parachutes at an angle of attack of zero deg. Overall drag was measured using an electrical force balance. The output of this balance was recorded simultaneously with the output of the Omega sensors. Figure 1 illustrates the orange parachute in the wind tunnel, fully inflated with Omega sensors attached to the canopy.

The Omega sensors were calibrated after attachment to the parachute. The parachute was then mounted in the wind tunnel and zero stress readings were taken with the parachute hanging freely. The parachute was then fully reefed at the base of the skirt and was uninflated at the start of the tests. The wind tunnel was run up to the desired dynamic pressure and the recording instrumentation was started. The parachute was disreefed and inflated rapidly. The test was continued until the Omega sensor outputs reached steady state. The wind tunnel was then shut down, the parachute was allowed to hang freely, and zero stress readings were again taken. Five tests were performed at each dynamic pressure. Tests were conducted at nominal dynamic pressures of 3.0, 5.3, and 7.1 psf (143.6, 253.8, and 340 Pa). A typical time history of these stresses and overall drag force is given in Fig. 2. All tests were performed at the infinite mass condition.

Results

Typical results from a series of five tests at constant dynamic pressure are shown in Fig. 3. The peak or maximum and steady-state stress are plotted as a function of nondimensional radial distance S^* from the apex of the parachute. Considering the variability inherent in the dynamics of solid parachutes, the data are remarkably uniform, particularly at steady state. The large data scatter at $S^* = 0.4$ is due to the fact that this sensor failed during the first test and after repair behaved somewhat erratically. Figure 3 was included to give an indication of the variation in results observed from test to test. In general, it would be hard to formulate any firm hypotheses about the basic physical mechanisms underlying the results by comparing one individual test to another. In this series of tests, for example, test 1 yielded the largest values of maximum stress; however, this effect was not noted in other test series conducted under exactly the same conditions and using the same test procedures. It is felt that the deviations from test to test are due primarily to the fact that the initial conditions are never exactly the same due to the highly turbulent nature of the flow around the parachute and to small variations in the disreefing sequence (a mechanical reefing line cutter was used). Once the reefing lines are cut, inflation is so rapid that these differences in initial conditions do not have time to smooth out; thus each test is somewhat unique. This hypothesis is supported by the much smaller variations observed at steady state and also by the fact that considerably less data scatter occurs during the inflation of ribbon parachutes (ribbon parachutes open much more slowly than do solid parachutes).

The steady-state stress distribution in the warp direction on the orange parachute is shown in Fig. 4 for three values of dynamic pressure. The small local maximum at an S^* of 0.6 disappears as dynamic pressure is increased and the stress reaches a maximum near the vent and near the skirt. At lower

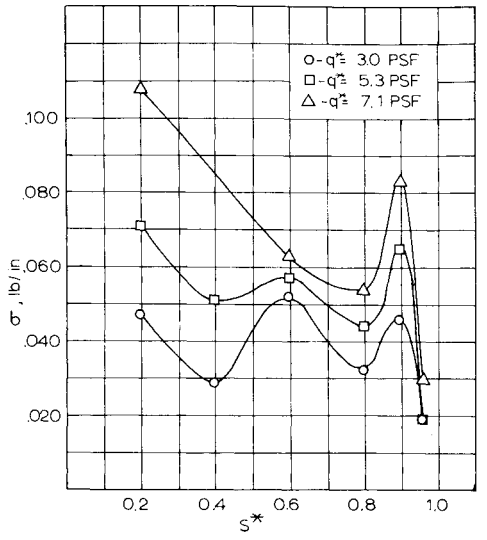

Fig. 4 Averaged steady-state stress distribution, orange parachute, warp direction.

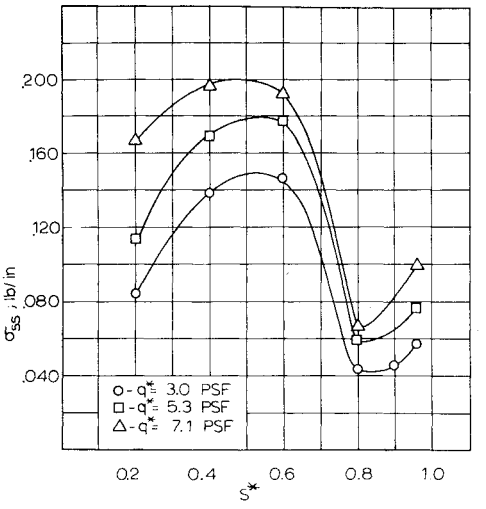

Fig. 6 Averaged steady-state stress distribution, orange parachute, fill direction.

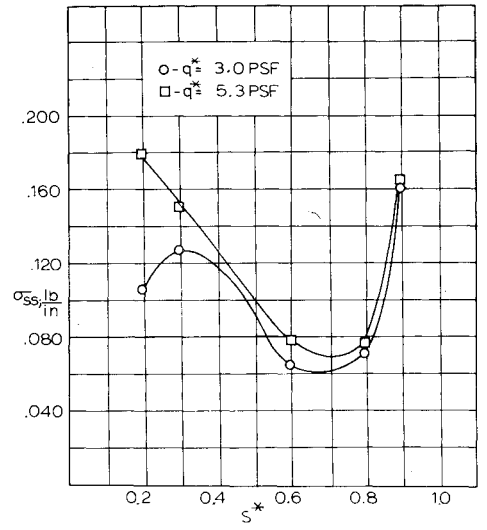

Fig. 5 Averaged steady-state stress distribution, white parachute, fill direction.

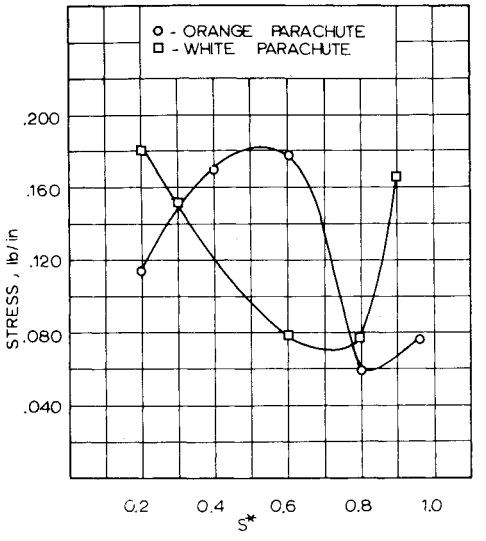

Fig. 7 Averaged steady-state stress distribution, fill direction at 5.3 psf (q^*).

dynamic pressure, the parachute canopy was not stretched tightly midway between the vent and the skirt and a number of local bulges and flat spots existed in this region. As dynamic pressure increased, these variations disappeared. Thus, stress measurement at intermediate values of S^* and lower values of dynamic pressure may be very much a function of the local geometry of the canopy at the Omega sensor location.

The steady-state stress distribution in the white parachute in the fill direction is shown in Fig. 5 for nominal dynamic pressures of 3.0 and 5.3 psf (143.6 and 253.8 Pa). Measurements were not made at 7.1 psf (340 Pa) because this parachute exhibited violent buffeting at this dynamic pressure. The Omega sensor mounted at an S^* of 0.96 failed during the testing and no data were obtained for this point. Although the general shape of the stress distribution curves are similar in the warp direction on the orange parachute and the fill direction on the white parachute, the magnitude of the stresses in the fill direction on the white parachute are about twice those in the warp direction on the orange parachute. This result was unexpected; therefore, six Omega sensors were mounted in the fill direction of the orange parachute and the tests were repeated. The results are summarized in Fig. 6. Although the distribution of fill stress is somewhat different in the orange and white parachutes, the magnitudes are about the same and are considerably greater than the warp stresses (Fig. 7).

Six sensors were mounted on each parachute at an S^* of 0.6. These sensors were mounted in different gores in order to determine the gorewise variation in stress. Steady-state measurements were taken on each parachute at the same dynamic pressure. The results of this investigation are shown in Table 1. One of the sensors on the orange parachute failed during the testing, thus only the results from five sensors are reported for this parachute. In order to provide a clear basis for comparing the two parachutes, the stresses were normalized with respect to the stress in gore 13 on the white parachute and gore 14 on the orange parachute. These are the gores from which the data shown in Figs. 3-7 were taken.

Since the numerical values of the stresses in the two parachutes were significantly different in magnitude, it was felt that the data should be normalized so that the two parachutes could be compared to one another. The data given in Table 1 represent the average of five tests. From an examination of the standard deviation of the data obtained from each sensor, it can be seen that the variations in

Table 1 Gorewise variation in stress, $S^* = 0.6$

White parachute						
Gore No.	1	5	9	13	17	21
Averaged normalized stress	1.865	0.878	1.524	1.000	0.500	1.036
Normalized standard deviation	0.098	0.146	0.268	0.220	0.085	0.134

Orange parachute						
Gore No.	1	3	8	14	17	21
Averaged normalized stress	0.632	0.618	1.324	1.000	1.015	Sensor failed
Normalized standard deviation	0.070	0.048	0.156	0.059	0.159	Sensor failed

	White parachute	Orange parachute
Mean value of normalized stress averaged across gores	1.133	0.918
Standard deviation of normalized stress across gores	0.442	0.226

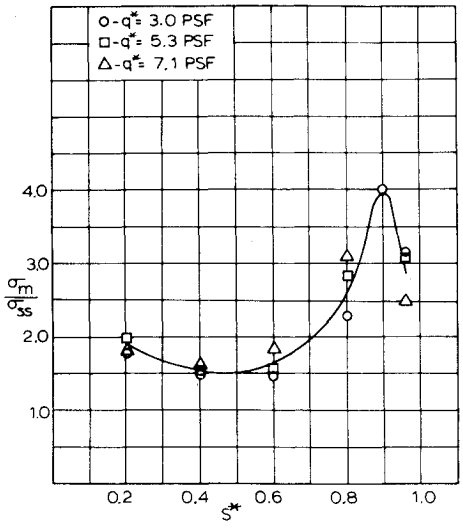

Fig. 8 Averaged ratio of maximum to steady-state stress distribution, orange parachute, fill direction.

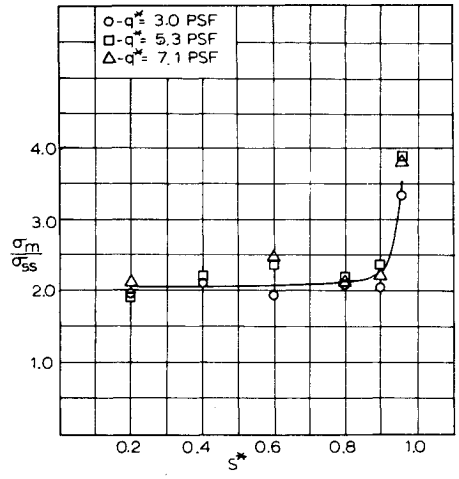

Fig. 9 Averaged ratio of maximum to steady-state stress distribution, orange parachute, warp direction.

measured stress from test to test are considerably less for the orange parachute than for the white parachute. This is because the white parachute exhibited considerable buffeting and localized flutter during testing, whereas the orange parachute did not. The value of the stress averaged across the gores is very near the nominal value in both parachutes; however, the variation from gore to gore is considerably greater in the white parachute than in the orange. This appears to be due to the fact that the construction of the orange parachute was much more uniform than that of the white parachute. When inflated, the white parachute exhibited a number of small localized bulges and wrinkles in the gores, whereas the gores in the orange parachute were very smooth. The erratic behavior of the white parachute appears to be due to irregularities in construction. This emphasizes the importance of careful construction techniques in parachute wind-tunnel models. Also, although the two parachutes were made from cloth with the same nominal properties, the actual material properties of the cloth used in constructing the two parachutes may have varied somewhat. Since the results obtained from the orange parachute were so much more uniform than those from the white parachute, all subsequent testing was performed on the orange parachute.

For the orange parachute, the ratio of maximum stress during inflation to steady-state stress is given in the warp direction in Fig. 8 and the fill direction in Fig. 9. This ratio is comparable to a local opening shock factor. These ratios are independent of dynamic pressure and increase rapidly near the skirt. Figures 10 and 11 indicate the ratio of the time of maximum stress to the time of maximum overall drag force as a function of S^* for both warp and fill directions in the orange parachute. Since the drag force measurements are made with a balance attached at the confluence point of the suspension lines, whereas the stress measurements are made on the canopy itself, it is not surprising that the measured time of maximum force lags the time of maximum stress. This same result has been reported for block-constructed parachutes in Ref. 2.

If the maximum stress during inflation was only a function of the maximum force, the maximum stress could be calculated by

$$\sigma_m = n\sigma_{ss}(F_m/F_{ss})$$

where n is equal to 1. The factor n can be determined from measured values and is plotted as a function of S^* for both warp and fill directions in Figs. 12 and 13. Since n is equivalent to dividing the local opening shock factor σ_m/σ_{ss} by the overall opening shock factor F_m/F_{ss}, a value of n equal

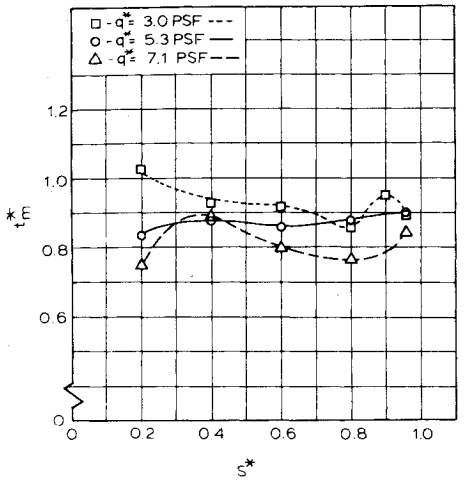

Fig. 10 Time of maximum stress along gore centerline, fill direction, $t_m^* = t_m / t_{f_m}$.

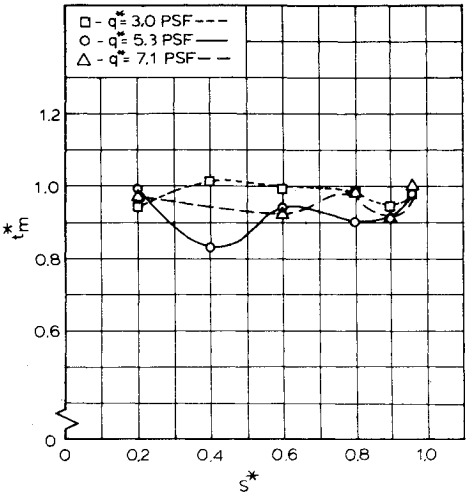

Fig. 11 Time of maximum stress along gore centerline, warp direction, $t_m^* = t_m / t_{f_m}$.

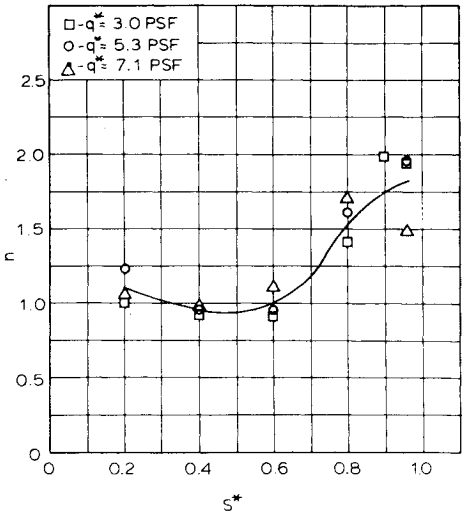

Fig. 12 Ratio of maximum stress to steady-state stress related to steady-state force and maximum force, fill direction $n = \sigma_m / \sigma_{ss} \cdot F_{ss} / F_m$.

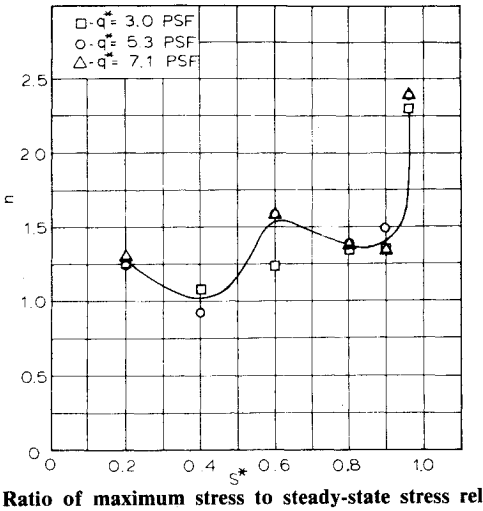

Fig. 13 Ratio of maximum stress to steady-state stress related to steady-state force and maximum force, warp direction $n = \sigma_m / \sigma_{ss} \cdot F_{ss} / F_m$.

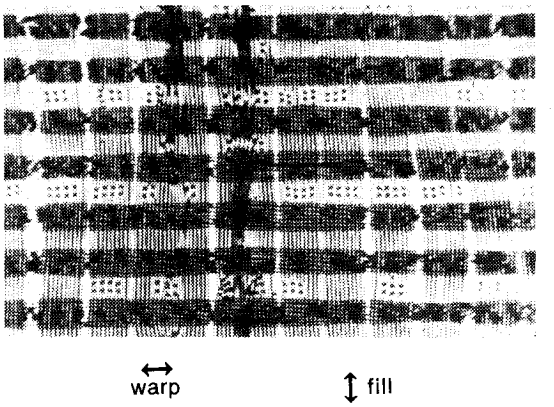

Fig. 14 Microscope picture (x40) of parachute canopy cloth.

to 1 would indicate that the maximum stress at any point in the canopy could be determined by multiplying the steady-state stress by the overall opening shock factor. The value of n is approximately 1 for values of S^* between 0.2 and 0.6, but increases to approximately 2.5 near the skirt.

This indicates that dynamic effects not directly related to maximum opening force influence maximum stress near the skirt, and simply multiplying the steady-state stresses by the overall opening shock factor may seriously underestimate maximum stress during inflation. It is interesting to note that n is relatively insensitive to dynamic pressure. Reference 2 shows n ranging from 1 to 2.5 for block-constructed, solid-flat parachutes and n ranging from 0.85 to 1.2 for ringslot parachutes.

Conclusions

The most important conclusion of this study is the fact that stress in the fill direction appears to be considerably larger than stress in the warp direction in bias-constructed, solid parachutes. A possible explanation for this is that the elastic properties of the parachute cloth are different in the warp and fill directions. Although initially the same, the warp and fill yarns are treated very differently during the process of weaving the cloth used for parachute canopies. The warp yarns undergo a mild acid treatment prior to weaving and are subjected to considerable tension during the weaving process. This may significantly change the elastic properties of these yarns. In addition, the fill yarns are intertwined among the warp yarns during weaving so that a force in the fill direction must not only elongate the fill yarns but also laterally displace the warp yarns. If the warp yarns are under tension, this could result in the fill direction being considerably stiffer than the warp direction.

Figure 14 is a microscopic photograph of the parachute cloth. The fact that the cloth is geometrically dissimiliar in the warp and fill directions is clear from this photograph. To completely test the hypothesis that the elastic properties of the cloth differ significantly in the warp and fill directions, it would be necessary to subject the parachute cloth to biaxial stress at stress levels and strain rates comparable to those measured in the inflating parachute canopies. Since these stress levels were very small, it was impossible to obtain even static biaxial stress/strain measurements with equipment available to the investigators. As noted in Ref. 7, it is very difficult to perform accurate biaxial stress/strain measurements on cloth at low stress levels. Static uniaxial stress/strain measurements were obtained, however, and these measurements indicated that at stress levels of the order of magnitude of those encountered during parachute inflation, the cloth was stiffer in the fill direction than in the warp direction. This finding gives some quantitative justification for the hypothesis that anisotropic stress/strain characteristics of the cloth account for the difference in the warp and fill stresses.

The fact that there appears to be significant variations in stress from gore to gore at a given radial distance from the vent indicates that in future studies of solid parachutes, simultaneous sets of stress measurements should be made on several gores so that the gorewise variation of stress at each S^* may be determined. Also, model parachutes should be constructed to be as uniform as possible so that localized variations in gore bulge radii are minimized. Since wind tunnel models are considerably less flexible than full-sized parachutes,[8] these localized variations appear to be much more important in wind tunnel models than in full-sized parachutes.

Acknowledgments

The research reported in this paper was supported by Sandia Laboratories under Contract No. 07-4328. Appreciation is given to the late Dr. H. G. Heinrich of the University of Minnesota who developed the Omega sensor and pioneered stress measurements in parachutes. Thanks are also due to D. Carey, D. Reynolds, and T. Weber, students at the University of Minnesota, who participated in this research.

References

[1] Heinrich, H. G. and Noreen, R. A., "Stress Measurements on Inflated Model Parachutes," Paper 73-445, AIAA 4th Aerodynamic Deceleration Systems Conference, Palm Springs, Calif., May 21-23, 1973.

[2] Heinrich, H. G. and Saari, D. G., "Parachute Canopy Stress Measurements at Steady State and During Inflation," *Journal of Aircraft*, Vol. 15, Aug. 1978, pp. 534-539.

[3] Heinrich, H. G., "Biaxial Stress Measurements on Cloth Samples and Bias Constructed Parachute Models," *Journal of Aircraft*, Vol. 17, July 1980, pp. 487-492.

[4] Wagner, P. M., "Experimental Measurement of Parachute Canopy Stress During Inflation," AFFDL-TR-78-53, May 1978.

[5] Braun, G. and Doherr, K. F., "Experiments with Omega Sensors for Measuring Stress in the Flexible Material of Parachute Canopies," *Journal of Aircraft*, Vol. 17, May 1980, pp.358-364.

[6] Eaton, J. A., "Improvement of the Temperature Characteristics of the Omega Sensor," IB 154-79/15, DFVLR—Institute fur Flugmechanik, Braunschweig, Federal Republic of Germany, Dec. 1979.

[7] Ewing, E. G., Bixby, H. W., and Knacke, T. N., "Recovery System Design Guide," AFFDL-TR-78-151, Dec. 1978, pp. 82, 208.

[8] Heinrich, H. G. and Hektner, R. J., "Flexibility as a Model Parachute Performance Parameter," *Journal of Aircraft*, Vol. 7, Sept. 1971, pp. 704-709.

From the AIAA Progress in Astronautics and Aeronautics Series . . .

VISCOUS FLOW DRAG REDUCTION—v. 72

Edited by Gary R. Hough, Vought Advanced Technology Center

One of the most important goals of modern fluid dynamics is the achievement of high speed flight with the least possible expenditure of fuel. Under today's conditions of high fuel costs, the emphasis on energy conservation and on fuel economy has become especially important in civil air transportation. An important path toward these goals lies in the direction of drag reduction, the theme of this book. Historically, the reduction of drag has been achieved by means of better understanding and better control of the boundary layer, including the separation region and the wake of the body. In recent years it has become apparent that, together with the fluid-mechanical approach, it is important to understand the physics of fluids at the smallest dimensions, in fact, at the molecular level. More and more, physicists are joining with fluid dynamicists in the quest for understanding of such phenomena as the origins of turbulence and the nature of fluid-surface interaction. In the field of underwater motion, this has led to extensive study of the role of high molecular weight additives in reducing skin friction and in controlling boundary layer transition, with beneficial effects on the drag of submerged bodies. This entire range of topics is covered by the papers in this volume, offering the aerodynamicist and the hydrodynamicist new basic knowledge of the phenomena to be mastered in order to reduce the drag of a vehicle.

456 pp., 6×9, illus., $25.00 Mem., $40.00 List

TO ORDER WRITE: Publications Dept., AIAA, 1290 Avenue of the Americas, New York, N.Y. 10104